Article

Innovative Plant-Derived Biomaterials for Sustainable and Effective Removal of Cationic and Anionic Dyes: Kinetic and Thermodynamic Study

El Mokhtar Saoudi Hassani [1,*], Dounia Azzouni [1], Mohammed M. Alanazi [2], Imane Mehdaoui [1], Rachid Mahmoud [1], Atul Kabra [3], Abdeslam Taleb [4], Mustapha Taleb [1] and Zakia Rais [1]

1   Laboratory of Engineering Electrochemistry, Modeling and Environment, Department of Chemistry, Faculty of Sciences Dhar Mahraz, Sidi Mohamed Ben Abdellah University, Fez 30000, Morocco; dounia.azzouni@usmba.ac.ma (D.A.); imane.mehdaoui@usmba.ac.ma (I.M.); rachid.mahmoud@usmba.ac.ma (R.M.); mustapha.taleb@usmba.ac.ma (M.T.); zakia.rais@usmba.ac.ma (Z.R.)
2   Department of Pharmaceutical Chemistry, College of Pharmacy, King Saud University, P.O. Box 2457, Riyadh 11451, Saudi Arabia; mmalanazi@ksu.edu.sa
3   University Institute of Pharma Sciences, Chandigarh University, Mohali 140413, Punjab, India; atul.e9963@cumail.in
4   Laboratory of Water and Environmental Engineering, Hassan II University of Casablanca, Casablanca 20150, Morocco; talebabdeslam1@gmail.com
*   Correspondence: saoudimokhtar94@gmail.com

Abstract: The aim of this study is to purify industrial textile effluents by treating two types of commonly encountered dyes: blue maxilon (BM), of cationic nature, and black eriochrome (NE), of anionic nature. We intend to employ an innovative approach based on the adsorption of these dyes onto a novel vegetal biomaterial derived from Aleppo pine fibers (FPAs). A kinetic and thermodynamic study was conducted. The effect of some physicochemical parameters on both dye adsorption and FPAs was also evaluated. The modeling of the adsorption results was performed using Langmuir, Freundlich, Temkin, and Dubinin Radushkevich (D-R) isotherms. The results indicate that the equilibrium time strongly depends on the initial concentration of the two dyes, being 60 min with pseudo-second-order adsorption kinetics for both dyes. Adsorption isotherms under the optimal conditions of adsorbent mass, temperature, medium pH, and dye concentration were used to determine the maximum adsorption efficiency, which was close to 93% and 98% for BM and NE, respectively. The results also show that the adsorption of both dyes on FPAs fits well with Langmuir's model. The thermodynamic study indicates that the adsorption of both dyes on FPAs is spontaneous and exothermic in nature for BM and endothermic for NE.

Keywords: cationic dye; anionic dye; Aleppo pine fiber; adsorption; kinetics; thermodynamic parameters

1. Introduction

In most developing countries, the industrial revolution constitutes a real threat and affects health and the environment in an alarming way [1]. Numerous studies have shown that the industries generating significant pollution in wastewater highly charged with pollutants [2] are those of textiles [3], tanneries [4], brass factories [5], and paper mills [6]. Indeed, these effluents are often loaded with little or non-biodegradable pollutants, in particular, certain dyes that are harmful to health [7] and lead to a very high level of pollution of surface water and groundwater [7,8]. According to the United Nations World Water Development Report (2017), dyes are carcinogenic, mutagenic, and teratogenic chemicals, and also toxic to humans and some species of fish and microorganisms [9].

Despite the implementation of certain programs in well-advanced countries in terms of environmental protection, and the efforts made by the Moroccan government to establish laws requiring industries, according to their activities, to equip themselves with wastewater

treatment units to reduce the pollutant load of effluents before they are discharged into watercourses via sewerage networks, the problem of surface water contamination by colored waters remains relevant and concerns the entire world [10].

Various methods have been developed for treating colored effluents, ranging from biological treatment [11,12] to coagulation/flocculation [13], chemical oxidation [11,14], membrane separation [15,16], and adsorption [17–38]. However, each method has potential drawbacks. For instance, biological treatment may be subject to specific constraints, such as the presence or absence of oxygen, and may be limited by the composition of the present dyes. In fact, coagulation/flocculation can lead to the formation of concentrated sludge, which may pose challenges in terms of disposal, particularly for high-flow effluents. In addition, chemical oxidation can be costly and energy-intensive, while membrane separation may require substantial investments in equipment and maintenance.

Adsorption is a widely used method in treating polluted waters due to its effectiveness and simplicity. It involves capturing dyes and pollutants with a solid material called an adsorbent. However, many traditional adsorbents, such as clays, zeolites, and activated carbons, may be costly to produce, originate from non-renewable natural deposits, and have limited regeneration capacity.

To address these challenges, many studies were focused on the development of alternative adsorbents that are biodegradable, affordable, and locally available from renewable natural resources or recyclable waste. These materials, such as biomass, agricultural residues, and industrial by-products, offer considerable potential for the sustainable treatment of colored effluents. So, by exploring these materials, we can discover multiple economical, ecological, and efficient solutions for industrial effluent treatment.

The objective of this study is to treat two dyes currently used in the textile industry, Maxilon Blue (BM) and Eriochrome Black T (NE), by adsorption on an innovative biomaterial derived from Aleppo pine fibers (FPAs). This biomaterial has never before been used to treat this type of pollution. The adsorption reaction time was determined by a kinetic study as a function of the BM and NE concentration of the dye solution, and pseudo-first- and pseudo-second-order models were used to correlate the kinetic data for dye adsorption on FPAs.

Operating conditions were optimized in terms of initial dye concentration, adsorbent mass, pH, and medium temperature for dye adsorption on the FPAs.

The results were modeled using Langmuir, Freundlich, Temkin, and D-R (Dubinin-Radushkevich) isotherms to understand the adsorption mechanism and determine thermodynamic parameters.

2. Materials and Methods

2.1. Adsorbent

The FPA powder was derived from the waste of Aleppo pine, supplied from the forest Ain chekaf ($33°59'43.476''$ N; $5°00'51.3''$ W) in the city of Fez in Morocco, and treated physically by dry cleaning, then dried in the oven for 12 h, followed by grinding and sieving to a particle size less than 1 mm. The obtained powder, named FPAs, was analyzed by measuring physicochemical parameters and spectroscopic analysis.

2.2. Adsorbate

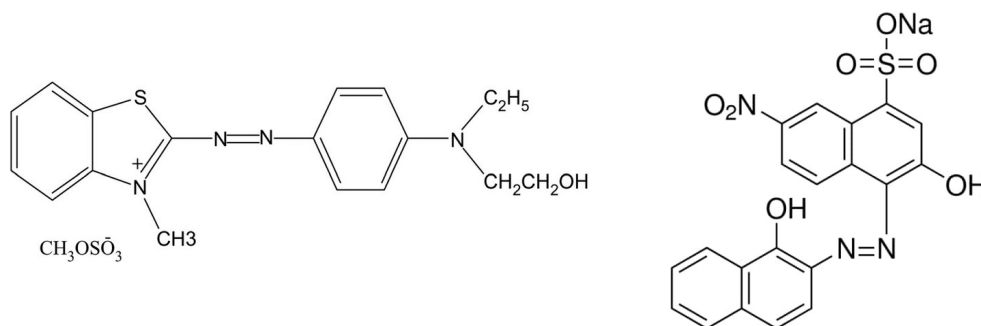Two dyes were used in this study: Eriochrome Black T (NE) and Maxilon Blue (BM).

NE is an anionic dye with a gross chemical formula $C_{20}H_{12}N_3O_7SNa$ and a solubility in water exceeding 50 g/L. It is characterized by the presence of chromophore groups (Vinyl (-C=C-), azo (-N=N-), and Nitro (-NO_2)), which is responsible for the colored aspect of the organic dyes due to the absorption of the ultraviolet rays, and of auxochrome groups, such as hydroxyl (-OH), which serve to enhance the effect of chromophore groups and ensure the solubility of dyes in water.

BM is a cationic dye with chemical formula $C_{19}H_{26}N_3O_6S_2$, characterized by the presence of chromophore groups Vinyl (-C=C-) and azo (-N=N-), and auxochromes groups Hydroxyl (-OH) (Table 1).

Table 1. Different characteristics of BM and NE.

Characteristics	Maxilon Blue	Eriochrome Black
Molecular weight (g/mole)	483	461.381
Chemical formula	$C_{19}H_{26}N_3O_6S_2$	$C_{20}H_{12}N_3O_7SNa$
Azo groups	Mono	Mono
Chromophore groups	(-N=N-) (-C=C-)	(-N=N-) (-C=C-) (-NO$_2$)
Auxochrome groups	(-OH)	(-OH)
Type	Cationic	Anionic
pH	5.6	5.6
λ_{max} (nm)	599	526
Chemical structure		

These dyes are widely used in laboratories as indicators for complexometric titrations and especially as dyeing dyes in textile industries because of their dye forms.

The 200 mg/L colored stock solution was prepared by dissolving 200 mg NE and BM in 1 L distilled water. The colored diluted solutions are produced by successive dilutions of the stock solution to obtain the solutions of different concentrations which will be used in the rest of this study.

Dye solutions before and after adsorption were analyzed by UV–Vis spectrophotometry of the UV-1800PC UV/VIS type, at wavelengths determined experimentally by scanning the wavelength spectrum between 400 nm and 900 nm for the different conditions studied (Figure 1).
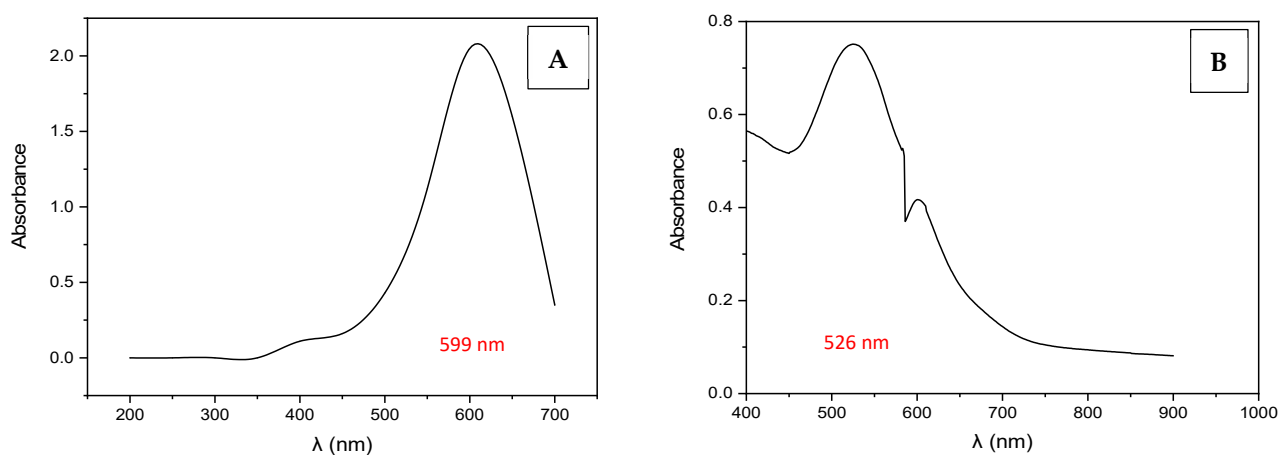

Figure 1. Adsorption maximum λ_{max} of BM (**A**) and NE (**B**) by UV/Visible spectroscopy.

2.3. Adsorption Process

2.3.1. Adsorption Kinetic

The kinetic study was performed on a suspension series of 0.05 g/L of FPAs in 100 mL of colored solutions with concentrations ranging from 5 to 120 mg/L. The mixtures were put under constant stirring of 300 rpm, at room temperature and pH of BM and NE solutions (5.8). Various samples were collected at various times, filtrated through a 0.45 μm PTFE syringe filter, and then analyzed by measuring the absorbance at the wavelength corresponding to the adsorption maximum, The adsorption capacity of the FPAs biomaterial was determined according to Equation (1):

$$Q_t = \frac{(C_i - C_t) \times \mathrm{V}}{\mathrm{m}} \tag{1}$$

where C_i (mg/L) is the initial dye concentration, C_t (mg/L) is the concentration of dye at time t, V (L) is the dye volume, and m (g) is the amount of adsorbent in the solution [19].

The results of the kinetic study were modeled according to the kinetic equations of pseudo-first-order (Equation (2)) or pseudo-second-order (Equation (3)) [20].

$$ln(q_e - q_t) = ln(q_e) - k_1 t \tag{2}$$

$$\frac{t}{q_t} = \frac{1}{k_2 q_e{}^2} + \frac{t}{q_t} \tag{3}$$

where q_e and q_t are, respectively, the amount of adsorbed material (mg/g) at equilibrium and at time t, k_1 (g/mg.h) is the first-order kinetic constant, and k_2 is the pseudo-second-order kinetic constant (g/mg.h).

The initial rate of adsorption, h, when $t = 0$ is defined by Equation (4):

$$h = k_2 \times q_e^2 \tag{4}$$

where q_e, h, and k_2 are calculated based on the slope and intercept of the t/q_t linear curve as a function of time.

The values of adsorption rate constants (k_2), initial velocities (h), and equilibrium adsorption capacities (q_e) are grouped in Table 4.

The results of the adsorption kinetics could be indicated on the identification of the diffusion mechanism by application of the intraparticle diffusion model given by Equation (5) after Webber and Morris [21].

$$Q_t = K_t.t^{\left(\frac{1}{2}\right)} + C \tag{5}$$

where K_t is the velocity constant of the intraparticle diffusion. The value of C indicates the boundary layer thickness. It corresponds to the intercept value.

In this model, if the curve of q_t versus $t_{1/2}$ (Figure 5) presents a straight line passing through the origin, the speed of the adsorption phenomenon is considered limited by the process of intraparticle diffusion [22].

2.3.2. Adsorption Isotherms

Adsorption isotherms explain how the adsorbate molecules distribute between the liquid and solid phases when the adsorption process reaches a steady state. They were determined by adding a mass of 5 mg to a series of 250 mL vials containing 100 mL of solutions with the same concentrations of the 2 dyes as used in the adsorption tests. The solutions were stirred at 300 rpm for the equilibrium time determined by the reaction kinetics at room temperature (20 ± 2 °C), keeping the pH of the medium constant. The isotherm models considered were those of Langmuir [33], Freundlich [34,35], Temkin [36], and Dubinin Radushkevich (D-R) [37], as they better describe the adsorption mechanism of organic dyes.

- The Langmuir model is an adsorption model based on the formation of a single layer of adsorbate on the surface of the adsorbent. It is represented by Equation (6) [23]:

$$\frac{C_e}{q_e} = \frac{C_e}{q_m} + \frac{1}{K_L \times q_m} \tag{6}$$

where q_e (mg/g) is the quantity of dye adsorbed at equilibrium, K_L is the Langmuir constant related to the affinity of the binding sites and the adsorption energy, and C_e is the concentration of the dye solution at equilibrium (mg/L)

Plotting C_e/q_e in a function of C_e allows us to determine q_m and K_L.

The most important characteristics of the Langmuir isotherm can be represented by the separation factor R_L [23,24], which can be calculated by Equation (7):

$$R_L = \frac{1}{1 + K_L C_0} \tag{7}$$

where K_L is the constant of the Langmuir isotherm and C_0 is the largest starting concentration (mg/L).

The confirmation of the R_L separation factor is based on the following criteria (Table 2).

Table 2. Adsorption types according to R_L values.

R_L	$0 < R_L < 1$	$R_L > 0$	$R_L = 1$	$R_L = 0$
Adsorption type	Adsorption is favorable	Unfavorable adsorption	Linear adsorption	Irreversible adsorption

The isotherm of Freundlich is presented by the linearized form the defined Equation (8) [23]. It supposes that adsorption takes place on the heterogeneous surface according to a multi-layer adsorption process and that the quantity adsorbed increases according to the concentration.

$$log q_e = log K_F + \frac{1}{n} log C_e \tag{8}$$

where K_F and n are the constants of Freundlich, and q_e is the maximum saturation adsorption capacity.

The intensity parameter values $1/n$ indicate the variation of the adsorption isotherm from linearity:

1. When $1/n = 1$, the absorption process is linear, which indicates a homogeneity of the sites and the absence of any interaction between the adsorbed species.
2. When $1/n < 1$, the adsorption process is favorable, the retention capacity increases, and many new adsorption sites appear.
3. When $1/n > 1$, the adsorption process is not favorable and the adsorption chains become weaker, resulting in a decrease in the adsorption capacity.

- The Temkin isotherm is represented by the following equation:

$$q_e = B_T Ln(C_e) + B_T Ln(K_T) \tag{9}$$

where B_T and K_T are the Temkin isotherm constants.

The Temkin isotherm contains a factor that takes the interactions between the adsorbent and the adsorbate explicitly into account (Table 3).

- The Dubinin–Radushkevich (D-R) isotherm model has been studied to take into consideration the effect of the porous structure of the adsorbents as well as their free energy of adsorption. It is expressed by the following equation [25]:

$$log(q_e) = log(q_{DR}) - K_{DR}\varepsilon^2 \tag{10}$$

where q_e (mg/g) is the quantity adsorbed on the adsorbent at the equilibrium, q_{DR} (mg/g) is the capacity of adsorbate adsorbed on the surface of the solid, K_{DR} (mol^2 KJ^{-2}) is the Sorption Energy Constant, and ε is the potential of Polanyi, defined by Equation (11):

$$\varepsilon = RTln\left[1 + \frac{1}{C_e}\right] \tag{11}$$

Table 3. Correspondence of the values of the constant B_T of the Temkin isotherm.

B_T	$B_T < 8$	$8 < B_T < 16$	$B_T > 16$
Adsorption process	Physical adsorption	Ion exchange	Chemical adsorption

The average adsorption energy E (kJ/mol) is obtained using the following equation [26]:

$$E = \frac{1}{\sqrt{2K_{DR}}} \tag{12}$$

The value of the average adsorption energy E can give useful information about the adsorption process (physical or chemical) from the D-R isotherm, physical adsorption ($E < 8$ KJ.mol^{-1}), ion exchange ($8 < E < 16$ KJ.mol^{-1}), and chemical adsorption ($E > 16$ KJ.mol^{-1}) [26].

3. Results and Discussions

3.1. Main Characteristics of the FPA Adsorbent Material

The FPA powder is acidic in character, with a porous appearance that facilitates the adsorption and fixation of dyes. It also has a zero charge point equal to 5.8 and a specific surface of 384 m$^2\cdot$g^{-1}. It is mainly composed of hydroxyl, carboxyl, amine functional groups, mineral compounds, and organic compounds, including cellulose and other mineral elements, which are Ca, Mg, Fe, Na, P, Al, K, Ni, and Mo.

3.2. Adsorption Kinetic

To fully understand the adsorption mechanisms of the two dyes BM and NE on FPAs, mixtures of different concentrations were stirred according to the contact time between adsorbent and adsorbate from 0 to 180 min with a mass of adsorbent of (0.05 g/L) at the residual dye pH. In fact, different samples were taken for analysis at regular times so that the decolorization yields of the solutions was determined in the function of the contact time (Figure 2).
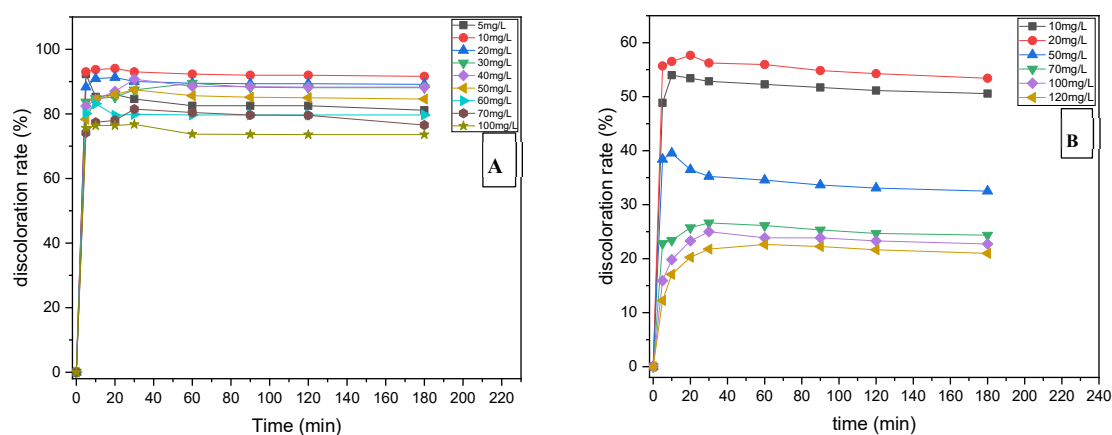
Figure 2. Adsorption kinetic of BM (**A**) and NE (**B**) on FPAs. Operating conditions: pH = 5.6, T = (20 ± 2) °C, adsorbent mass = 0.05 g/L.

For both dyes, the removal rate shows an increase with the reaction time following two different slopes. During the first one, a rapid increase of the decolorization yield is

noticed at the first 10 min for all the studied concentrations of the 2 dyes. At this time, the dyes adsorb first on the easily accessible adsorbent sites. In contrast, the second stage is characterized by a slowing down of the adsorption efficiency to a maximum value corresponding to the equilibrium time of 60 min for both dyes. This can be expressed by the diffusion of the dye to the less accessible adsorption sites until an adsorption equilibrium is reached.

Modeling of Adsorption Kinetic

It took place through the pseudo-first-order (PPO) and pseudo-second-order (PSO) models.

a.　　Pseudo-first-order kinetics (PPO)

With this model, the rate of adsorption at time t is considered proportional to a difference between the equilibrium adsorbed amount Q_e and the amount Q_t adsorbed at that instant; the adsorption process is reversible [27].

The constants of the pseudo-first-order kinetics were determined by plotting the $\log(q_e-q_t)$ versus the timeline of the different studied concentrations (Equation (2)). The values of the first-order constants K_1, the theoretical and experimental quantities, and the coefficient of determination R^2 of the studied concentrations of BM and NE are presented in Table 4.

Table 4. Adsorption kinetic constants of BM and NE on FPAs.

Kinetic Model	Pseudo-First-Order					Pseudo-Second-Order			
Concentration (mg/L)	R^2	K_1 (min^{-1})	qe_{the} (mg/g)	qe_{exp} (mg/g)	R^2	K_2 (g/mg.min)	h (mg/g.min)	qe_{the} (mg/g)	qe_{exp} (mg/g)
BM									
5	0.04	0.0003	1.314	8.25	0.99	−0.015	**−0.126**	8.123	8.25
10	0.02	0.003	0.587	18.46	1	−0.188	**−3.472**	18.31	18.46
20	0.05	0.005	1.33	35.80	1	−0.148	**−5.312**	35.71	35.80
30	0.45	0.014	4.76	53.71	1	0.099	**5.322**	52.91	53.71
40	0.25	0.011	6.436	70.84	1	0.221	**15.65**	70.92	70.84
50	0.11	0.007	7.133	85.63	0.99	0.049	**4.192**	84.74	85.63
60	0.03	0.004	6.099	95.61	1	−0.110	**−10.51**	95.23	95.61
70	0.08	0.007	7.458	112.60	0.99	−0.011	**−1.261**	108.69	112.60
100	0.02	−0.004	3.34	147.43	1	−1.492	**−219.96**	147.05	147.43
NE									
10	0.03	−0.002	0.394	10.45	0.99	−0.125	**−1.306**	10.13	10.45
20	0.17	−0.006	0.368	22.39	0.99	−0.044	**−0.985**	21.41	22.39
50	0.61	−0.01	1.85	34.55	0.99	−0.017	**−0.587**	32.36	34.55
70	0.07	0.003	1.719	36.59	0.99	−0.028	**−1.024**	34.24	36.59
100	0.05	0.004	4.86	47.73	0.99	−0.074	**−3.532**	46.08	47.73
120	0.20	0.009	6.35	53.32	0.99	0.042	**2.239**	51.51	53.32

The results of the R^2 values of both dyes are low and the theoretically adsorbed amounts (q_{the}) are also very low compared to the experimentally adsorbed amounts of both dyes. These observations indicate that the adsorption of BM and NE on FPAs does not correspond with a diffusion-controlled process since it does not satisfy the pseudo-first-order equation.

b.　　Pseudo-second-order kinetics (PSO)

The graph of t/Q_t versus t in Equation (3) is linear (Figure 3), implying that the adsorption of the two dyes on the FPAs has pseudo-second-order kinetics.
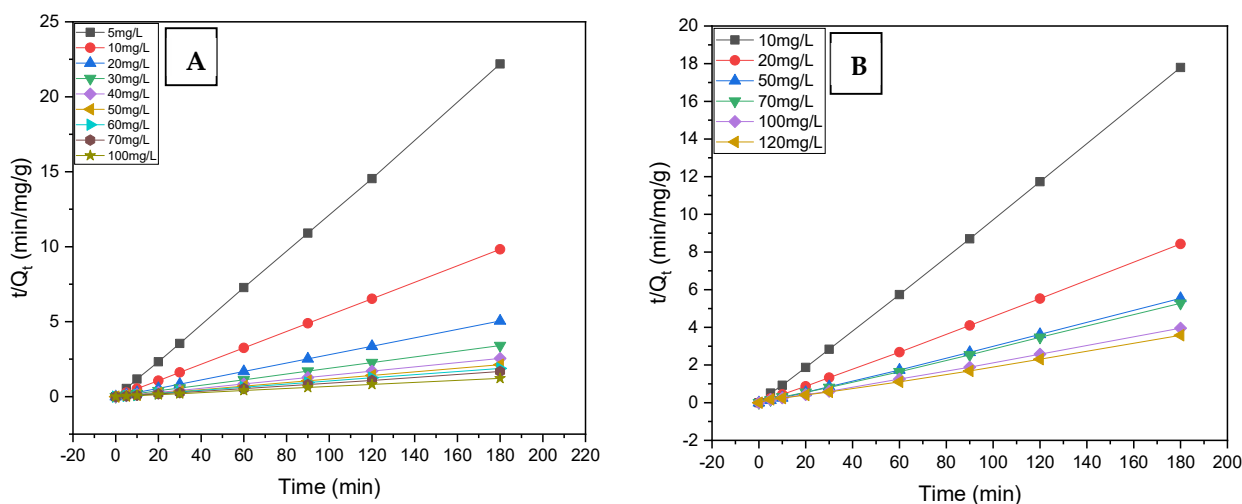
Figure 3. Application of the pseudo-second-order model for the adsorption of BM (**A**) and NE (**B**) on FPAs.

The adsorbed quantities q_e, the constants of this model K_2, and the regression coefficients R^2 of all employed concentrations are given in Table 4.

The results show that the equilibrium adsorbed amount q_e increases with the increasing initial concentration of both dyes. In addition, the values of the linear regression correlation coefficient R^2 for the second-order model are higher than those for the first-order model, and they are very close to 1 for all studied concentrations of both dyes. In addition, the theoretically adsorbed quantities (q_{the}) are very close to the values found experimentally and closer to those calculated using the second-order kinetics model.

All the results indicate that the adsorption kinetics of BM and NE on FPAs are perfectly defined by the pseudo-second-order kinetic model whatever the concentration of the dye solution is. This model considers chemisorption as the step that involves electron exchange and hydrogen bonding at the solid–liquid interface (Figure 4).
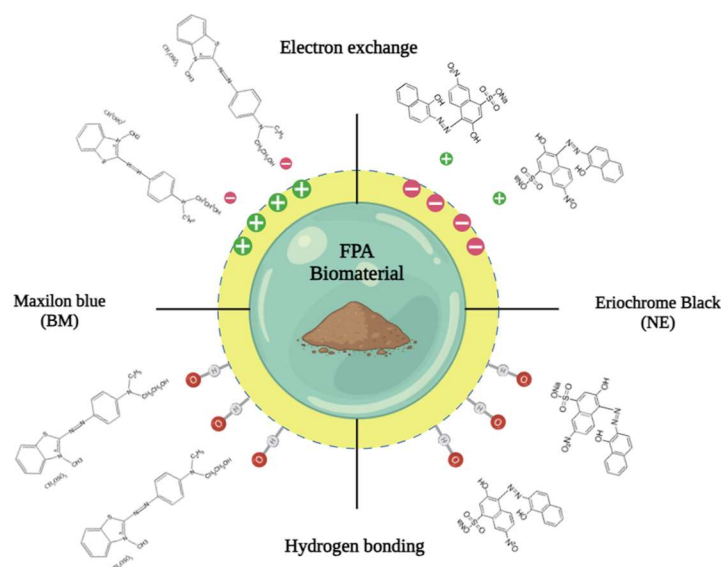

Figure 4. Chemical adsorption mechanism of BM and NE on FPA biomaterial.

When dyes come into contact with the biomaterial surface, electrostatic interactions occur, leading to electron transfer between dye molecules and active sites on the adsorbent surface. These electrostatic interactions can be enhanced by the presence of functional groups on the adsorbent surface, which can accept or donate electrons to form chemical bonds. At the same time, hydrogen bonds can form between the dye molecules and the

adsorbent's functional groups. Hydrogen bonds are weak but significant interactions that occur between a partially positively charged hydrogen atom and a partially negatively charged oxygen, nitrogen, or sulfur atom in another molecule. These bonds can stabilize the dye molecules on the adsorbent surface and promote their adsorption. These electrostatic interactions and hydrogen bonds between the adsorbent and adsorbate contribute to the attachment of dyes to the biomaterial surface and play a decisive role in the adsorption kinetics described by the pseudo-second-order model.

The initial equilibrium adsorption rate calculation showed that the reaction rate is highly dependent on the dye concentrations (BM and NE).

These results imply that the BM and NE molecules adsorb onto the active sites of the FPAs with varying rates depending on the initial dye concentration.

3.3. Adsorption Mechanism

The adsorption of BM and NE dyes onto FPAs can be described in three successive steps. First, the dyes migrate through the solution to the outer surface of the FPA particles. Next, the dyes move inside the particles, and finally, they adsorb onto free positions on the inner surface of the adsorbent.

The representation of the adsorption capacities of the biomaterial as a function of the square root of t (Figure 5) is multilinear whatever the concentration of the solution and represents very low values of correlation coefficients R^2 and all lower than 0.59.
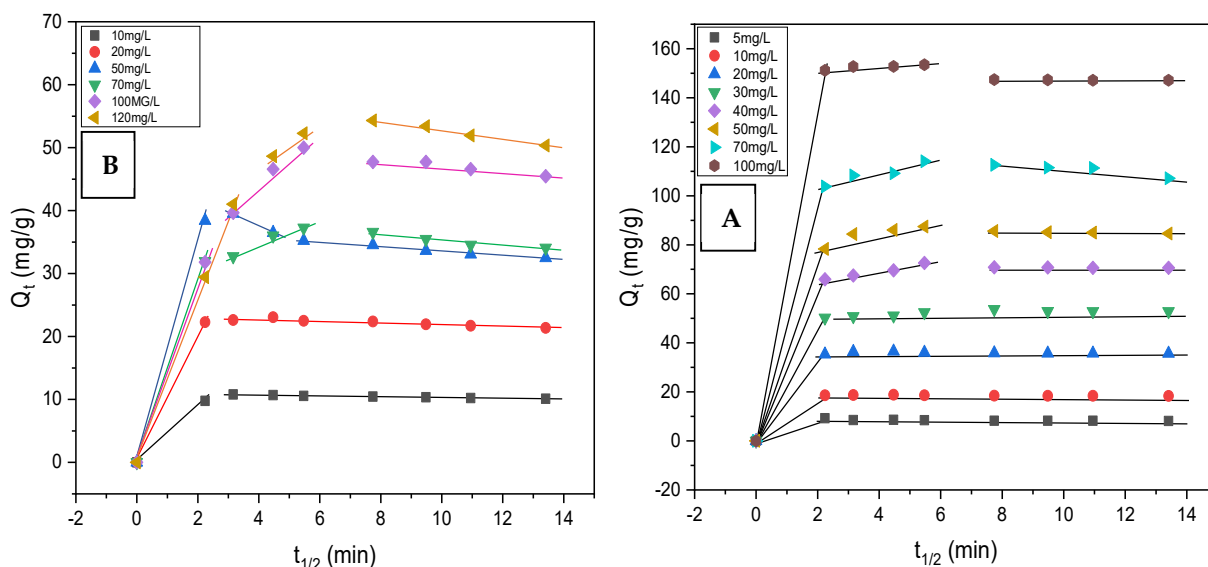

Figure 5. Intraparticle diffusion model for the adsorption of BM (**A**) and NE (**B**) on FPAs.

In the beginning, the dye adsorbs on the external surface of the FPA particles at a slightly faster speed for all the studied concentrations of the two dyes except for the first two concentrations of BM, which adsorb slowly. Until saturation of the external surface of the FPAs, at this time the dye molecules penetrate and adsorb on the internal surface of the FPAs. This increases the resistance to diffusion and subsequently leads to a decrease in the diffusion rate. As the dye concentration in the solution decreases, the rate of diffusion becomes lower and lower.

The intraparticle diffusion constants (K_t and C) results calculated from Equation (5) (Table 5) show that these constants (K_t and C) are different from zero and increase with dye concentration, confirming that intraparticle diffusion is not the only mechanism limiting the adsorption process of the two dyes BM and NE on FPAs.

Table 5. Parameters related to the intraparticle mechanism of the two dyes on FPAs.

Concentrations Mg/L	Diffusion Constants		
	K_t	C	R^2
BM			
5	0.4769	5.136	0.2116
10	1.1935	10.513	0.2795
20	2.366	20.074	0.293
30	3.7704	27.481	0.3516
40	5.0734	36.684	0.354
50	5.9913	45.212	0.3361
70	7.6828	59.136	0.3285
100	9.3354	86.575	0.261
NE			
10	0.678	5.827	0.2863
20	1.3617	12.951	0.2521
50	1.6705	23.138	0.1442
70	2.5038	18.441	0.3411
100	4.0568	19.223	0.4935
120	4.9886	17.431	0.5922

3.4. Adsorption Isotherms

Figure 6 shows the curves of the quantity of adsorbate retained per gram of the adsorbent in the function of the equilibrium adsorbate concentrations of BM and NE. The shape of the BM curve indicates that as the initial concentration of dye increases, the quantity of the adsorbed dye on the adsorbent also increases to the steady state, reflecting that the interactions between the adsorbate and the adsorbent are greater than that between the adsorbate molecules. This minimizes adsorption site competition between the adsorbent and the dyes to promote monolayer adsorption.
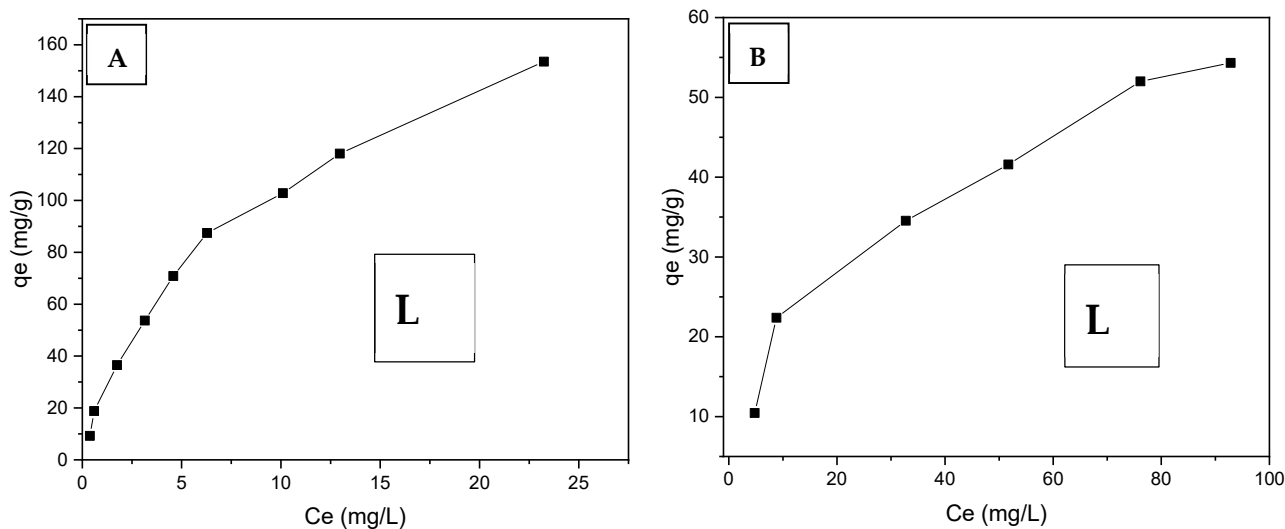

Figure 6. BM (**A**) and NE (**B**) adsorption isotherms on FPAs in aqueous solutions. Operating conditions: pH = 5.6, T = (20 ± 2) °C, adsorbent mass = 0.05 g/L.

Based on the Giles et al. [28] classification, the adsorption isotherms of BM and NE on FPAs are of type L.

The L-type isotherm for both BM and NE dyes indicates that the number of vacant sites decreases as the equilibrium concentration increases. This type of isotherm reflects the high affinity of the adsorbate/adsorbent. The solutes can be adsorbed horizontally on the surface of the adsorbent or vertically, which minimizes the competition of adsorption sites between the adsorbent and the dyes. The shape of the adsorption curve is characteristic

of the chemical adsorption process, the isotherm can then be modeled by the Langmuir equation [29].

3.5. Optimization of Adsorption Parameters

The parameters influencing the adsorption phenomenon are the dye solution concentration, the pH, the temperature of the medium, and the mass of the adsorbent. Each optimized parameter is taken into consideration for the further optimization of the other parameters. The tests were performed on 100 mL solutions of the dyes at pH and temperature T. These mixtures were stirred with a speed of 300 rpm during the equilibrium time determined by the adsorption kinetics (60 min). The residual concentrations were determined by UV–Visible spectrophotometry and then exploited in order to follow the evolution of the adsorption yield of the dyes according to the values of the studied parameter.

3.5.1. Dye Solution Concentration Effect

The effect of the initial dye concentration was studied under the same conditions as before, this time changing the concentrations from 10 to 120 mg/L. The evolution of the decolorization yield according to the concentration of the dye (Figure 7) shows that for BM, the highest yield (93%) is reached for the concentration of 70 mg/L.
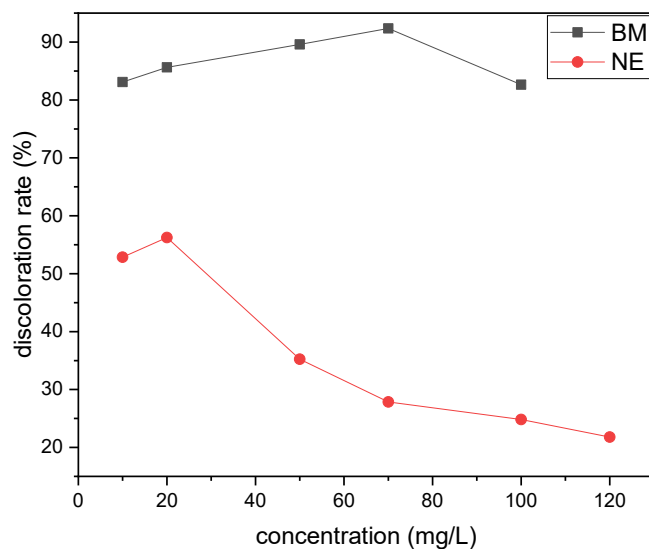

Figure 7. Initial dye concentration effect (BM and NE) on adsorption efficiency of FPAs. Operating conditions: pH = 5.6, T = (20 ± 2) °C, adsorbent mass = 0.05 g/L, (BM) = 10, 20, 50, 70 and 100 mg/L, (NE) = 10, 20, 50, 70, 100 and 120 mg/L, stirring time = 60 min.

For the NE, it is 57% for the concentration of 20 mg/L. Above these concentrations, these yields decrease because of the saturation of the sites active on the surface of the FPAs in the presence of a high dye content [30].

3.5.2. Adsorbent Mass Effect

The initial adsorbent mass effect was evaluated from 0.1–3 g/L and at optimum concentrations of 70 and 20 mg/L of BM and NE, respectively, while keeping other parameters constant.

The decolorization efficiency of both dyes changed with the increasing mass of the adsorbent used (Figure 8). Indeed, a mass of 1.5 g/L of FPAs is likely to adsorb a maximum of 94 and 69% of BM and NE, respectively. This phenomenon is the result of an increase in the number of sites available for dye binding, which consequently favors the phenomenon of discoloration [31–39]. Above this mass, the adsorption power decreases slightly, probably revealing the presence of other types of interactions between the dyes and the FPAs, or a

competition between the sites retaining the dye molecules and the free sites of the adsorbent which attract them back into the solution.
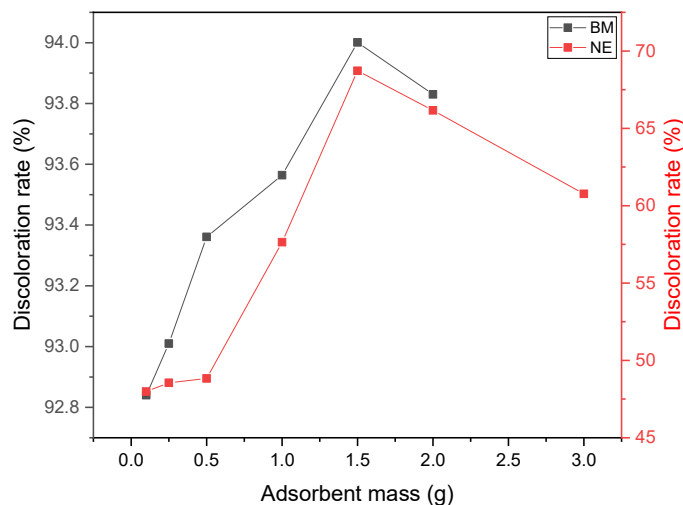

Figure 8. Effect of adsorbent mass on the adsorption efficiency of dyes (BM and NE) on FPAs. Operating conditions: pH = 5.6, T = (20 ± 2) °C, Adsorbent mass = 0.1 à 3 g/L, concentration NE = 20 mg/L, BM = 70 mg/L, stirring time: 60 min.

3.5.3. Medium pH Effect

We studied the impact of pH by setting the optimum concentrations and mass of the adsorbent and changing the solution pH from 2.5 to 10. Figure 9 shows that at an acid pH (3) below the FPAs' zero charge point value (pHzc = 5.9), the adsorption efficiency of NE reaches a maximum of 91% discoloration and a minimum of 54% for BM. At this acidic pH, the FPAs' surface is predominantly positively charged and can interact with negative species, favoring the adsorption of the anionic dye (NE) more than the cationic dye (BM). Consequently, at a solution pH above 5.9, the FPAs' surface is predominantly negatively charged and can interact with the cationic dye (BM), demonstrating the maximum decolorization efficiency of BM (93%) at pH = 7.5 and the decreased decolorization efficiency of NE (20%). It was highest (92%) at pH = 3.
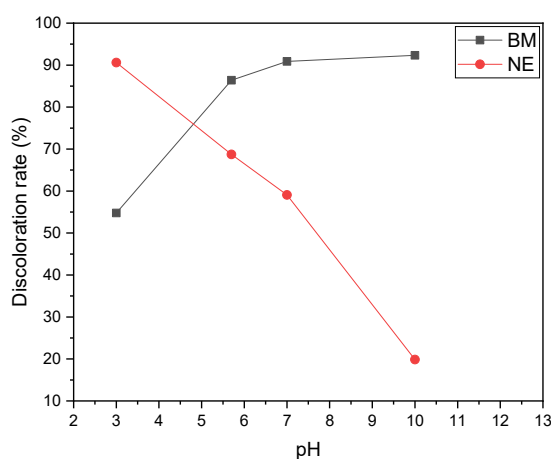

Figure 9. Effect of the pH solution on the adsorption efficiency of BM and NE on FPAs. Operating conditions: T = (20 ± 2) °C, adsorbent mass = 1.5 g/L, NE concentration = 20 mg/L, BM = 70, 3 ≤ pH ≤ 10, stirring time = 60 min.

3.5.4. Medium Temperature Effect

The effect of temperature on the rate of decolorization of the two dyes by FPAs was ensured by a series of experiments conducted at temperatures of 20, 30, 40, and 60 °C.

The results in Figure 10 show an increase of 3% for NE up to a temperature of 40 °C with a discoloration efficiency of 98%. For BM, the increase in temperature hinders its adsorption on the FPAs.
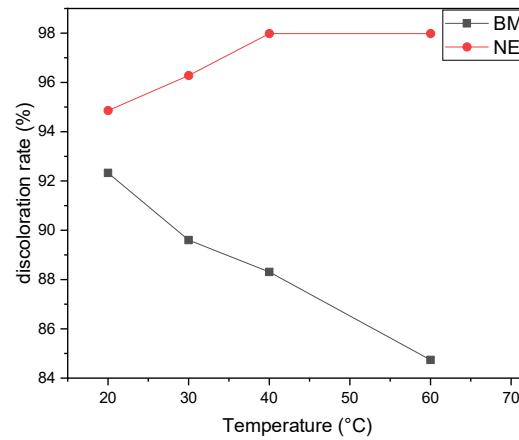

Figure 10. Medium temperature effect on the adsorption efficiency of BM and NE on FPAs. Operating conditions: pH (BM) = 10, pH (NE) = 3, adsorbent mass = 1.5 g/L, [NE] = 20 mg/L, [BM] = 70, $10 \leq T°C \leq 60$, stirring time = 60 min.

3.6. Modeling of Adsorption Isotherms

To optimize the process of adsorption, four models of adsorption isotherms are studied: Langmuir, Freundlich, Temkin, and Dubinin–Radushkevich in their linear form as shown in Figure 11.
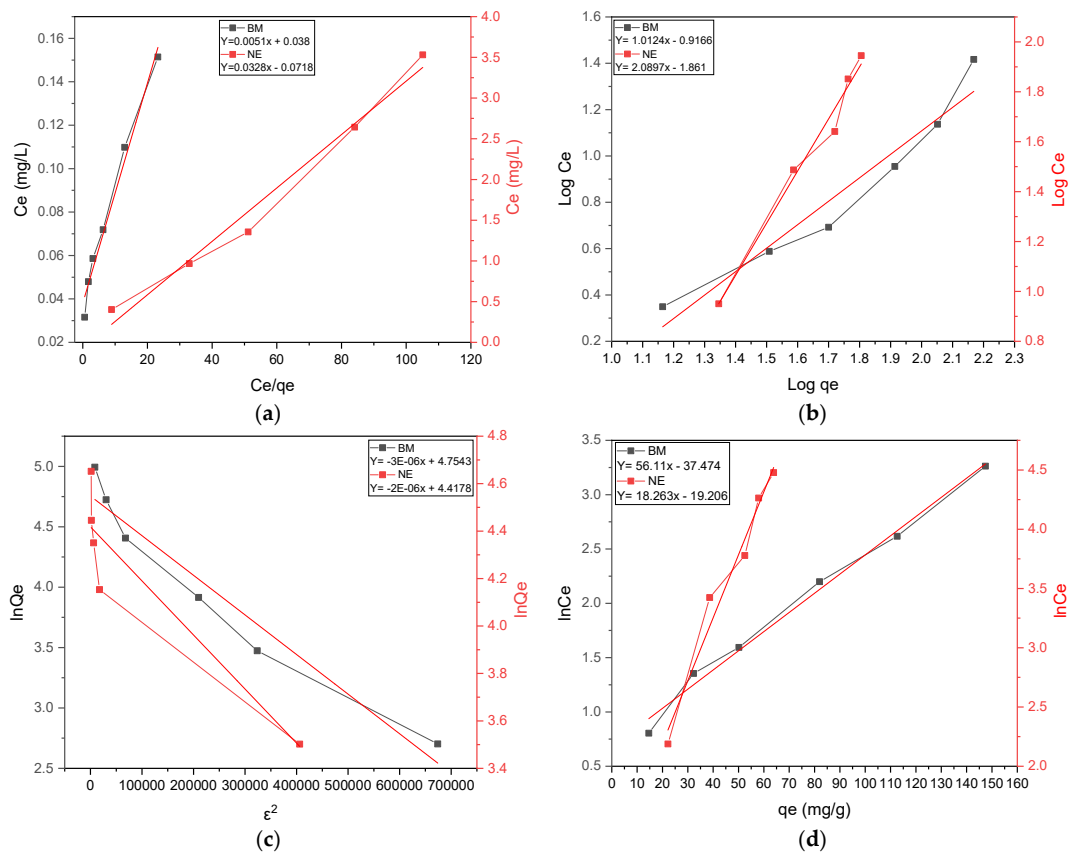

Figure 11. Linear representation of Langmuir (**a**), Freundlich (**b**), D-R (**c**), and Temkin (**d**) isotherms for the adsorption of BM and NE on FPAs.

The parameters of equilibrium and the constant values of the four isotherms were determined by linear regression (Table 6).

Table 6. Langmuir, Freundlich, Temkin, and Dubinin–Radushkevich parameters of BM and NE adsorption on FPAs.

Dyes	Langmuir			Freundlich			Temkin			D-R		
	(mg/g)	R^2	1/n		R^2	B_T	K_T	R^2	K_{DR}	E (Kj/mol)	R^2
BM	196.078	0.134	0.983	1.124	0.143	0.941	56.11	5.31×10^{-17}	0.991	3×10^{-6}	4.08×10^2	0.860
NE	30.488	−0.457	0.981	2.088	0.014	0.981	18.26	4.56×10^{-9}	0.970	2×10^{-6}	5×10^2	0.857

The results of modeling the adsorption isotherms of the two dyes BM and NE on FPAs record that the retention process of these dyes are both described by the Langmuir and Temkin models. Indeed, the coefficients of determination for the 2 isotherms are close to 1 for both dyes and the values of Langmuir's R_L separation factor for the different concentrations of BM and NE (Table 7) are between 0 and 1, which confirms the validity of this model. The numerical values of K_F and $1/n$ for both dyes (Table 6) do not meet the validation criteria of the Freundlich model.

Table 7. Separation factor for different concentrations of BM and NE dyes.

C (mg/L) R_L	10	20	30	50	70	100	120
BM	0.427	0.271	0.199	0.131	0.097	0.07	-
NE	-	0.89	-	0.96	0.97	0.98	0.98

As for Temkin's model, it shows that there is no complex formation (K_T is very low) or interaction between adsorbed molecules, and the adsorption reaction is exothermic for the NE at the substitution of one or more water molecules by the dyes. This reinforces the Langmuir model that is based on the non-interaction between entities adsorbed on sites of the same nature.

These results can be explained by a monolayer adsorption characterizing the Langmuir isotherm, without any dye–dye interaction and without complex formation.

The average free energy E (kJ/mol) values for both dyes, provided by the K_{DR} constant calculation of the Dubin–Radushkevich isotherm (Table 6) are greater than 16 kJ/mol, revealing that the adsorption of both dyes is chemical in nature, which is also proven by the B_T values obtained from the Temkin isotherm ($B_T > 16$).

3.7. Thermodynamic Study

The nature of adsorption of BM and NE dyes on FPAs powder was evaluated by calculating the thermodynamics parameters standard free energy (ΔG°) (J/mol), standard enthalpy (ΔH°) (J.mol^{-1} K^{-1}), and standard entropy (ΔS°) (J/mol) (Table 8) according to the following equations [32]:

$$K_d = \frac{Q_e}{C_e} \tag{13}$$

$$\Delta G° = -RT.lnK_d \tag{14}$$

$$lnK_d = \left(\frac{\Delta S°}{R}\right) - \left(\frac{\Delta H°}{R}\right)\frac{1}{T} \tag{15}$$

where K_d is the Distribution Constant deduced from the adsorption capacity Q_e (mg/g) of the FPA adsorbent, and C_e (mg/L) is the equilibrium concentration.
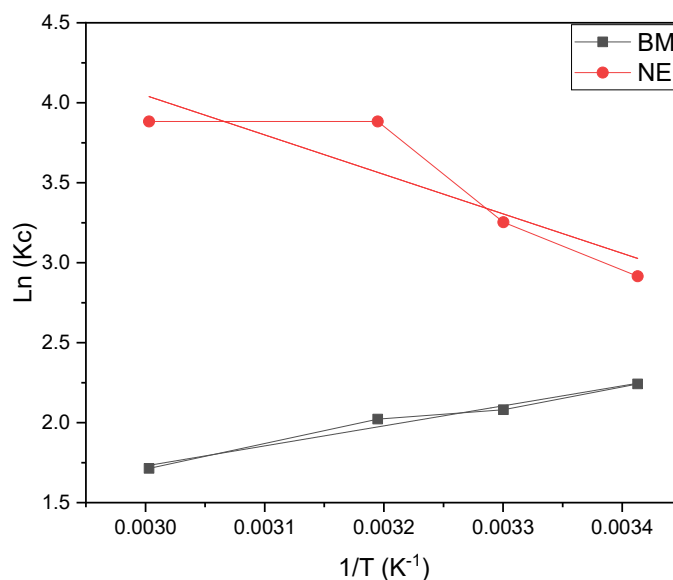
Table 8. Thermodynamic parameters of adsorption of BM and NE on FPAs.

Parameters	Temperatures	ΔH° (J.mol^{-1} K^{-1})	ΔS° (J/mol)	ΔG° (J/mol)
BM	20 °C	−10,409	−16.85	−5460.406028
	30 °C			−5242.206332
	40 °C			−5261.755284
	60 °C			−4745.671639
NE	20 °C	20,518.9	95.19	−7100.774357
	30 °C			−8195.002824
	40 °C			−10105.07668
	60 °C			−10750.76848

R: constant of perfect gases (J.mol^{-1} K^{-1}) (8.314 J mol^{-1} K^{-1})

T: temperature absolute (K)

The results shown in Figure 12 demonstrate that BM adsorption on FPAs is exothermic in nature ($\Delta H^\circ < 0$), while NE adsorption is endothermic ($\Delta H^\circ > 0$), meaning that increasing temperature increases the adsorbent's maximum carrying capacity at the same time. However, the negative value of ΔS° in the case of BM adsorption on FPAs, shows that the distribution order of the dye molecules on the adsorbent is important compared to that in the solution, while the positive value of ΔS° of NE suggests that some structural changes are taking place on the adsorbent and reveals the presence of random interferences at the solid-liquid interface. On the other hand, the negative values of ΔG° indicate that the adsorption process for both dyes is spontaneous throughout the temperature range studied. We also note that for BM, ΔG° increases with increasing solution temperature, which may be explained by the fact that adsorption becomes somewhat more difficult as temperature rises. As for NE, ΔG° values decrease with increasing solution temperature, which can be explained by the fact that NE adsorption is more favorable at high temperatures [33].

Figure 12. Linear representation of the variation of Ln (K$_c$) as a function of 1/T for the adsorption of BM and NE on FPAs.

This confirms the results obtained for the temperature effect on the adsorption of both dyes on FPAs (Figure 10).

4. Conclusions

This study focused on the adsorption of the dyes Maxilon Blue (BM) and Eriochrome Black (NE) on Aleppo pine fiber powder (FPAs). The results obtained concerning kinetics,

adsorption isotherms, and thermodynamics were used to explain the way in which the two dyes attach to the adsorbent. A study of the influence of the initial concentration of the two dyes on the kinetics showed that the equilibrium time is 60 min and follows the pseudo-second-order model for both dyes. In addition, the adsorption parameter optimization study revealed that BM adsorption is more favored at basic pH with an adsorbent mass of 1.5 g/L and decreases with increasing temperature. NE adsorption, on the other hand, is favored at an acidic pH and a temperature of 40 °C. These two parameters give BM and NE removal rates of 93% and 98%, respectively. A study of the adsorption isotherms revealed that the binding of dye molecules to the active sites of the adsorbate was determined by monolayer adsorption characterizing the Langmuir isotherm, with no dye–dye interaction and no complex formation justified by the Temkin isotherm. The mean free energy (E) and constant (B_T) values determined from adsorption isotherms and D-R and Temkin, respectively, showed that the adsorption of both dyes on FPAs is chemical in nature. Thermodynamic parameters showed that the adsorption of BM and NE on FPAs is exothermic and endothermic in nature, respectively, and spontaneous throughout the temperature range studied.

In conclusion, the FPAs biomaterial recorded efficiency in the treatment and removal of cationic and anionic dyes typically used in textile industries with very interesting yields. These results recommend and suggest its application on an industrial scale.

Author Contributions: This article was a collaborative effort. E.M.S.H. supervised practical tasks, writing, and presentation of results, and handled the submission of the article. D.A., I.M. and R.M. contributed to practical tasks and results processing. M.M.A. provided funding, writing and reviewing. A.K. contributed to the interpretation of results. A.T. and M.T. supervised and verified the results. Z.R. guided supervised, and ensured the validity of results. All authors have read and agreed to the published version of the manuscript.

Data Availability Statement: Data are contained within the article.

References

1. Stearns, P.N. *The Industrial Revolution in World History*; Routledge: London, UK, 2020.
2. Kishor, R.; Purchase, D.; Saratale, G.D.; Saratale, R.G.; Ferreira, L.F.R.; Bilal, M.; Chandra, R.; Bharagava, R.N. Ecotoxicological and health concerns of persistent coloring pollutants of textile industry wastewater and treatment approaches for environmental safety. *J. Environ. Chem. Eng.* **2021**, *9*, 105012. [CrossRef]
3. Madhav, S.; Ahamad, A.; Singh, P.; Mishra, P.K. A review of textile industry: Wet processing, environmental impacts, and effluent treatment methods. *Environ. Qual. Manag.* **2018**, *27*, 31–41. [CrossRef]
4. Hansen, É.; de Aquim, P.M.; Hansen, A.W.; Cardoso, J.K.; Ziulkoski, A.L.; Gutterres, M. Impact of post-tanning chemicals on the pollution load of tannery wastewater. *J. Environ. Manag.* **2020**, *269*, 110787. [CrossRef] [PubMed]
5. Ndimele, P.E.; Pedro, M.O.; Agboola, J.I.; Chukwuka, K.S.; Ekwu, A.O. Heavy metal accumulation in organs of Oreochromis niloticus (Linnaeus, 1758) from industrial effluent-polluted aquatic ecosystem in Lagos, Nigeria. *Environ. Monit. Assess.* **2017**, *189*, 255. [CrossRef] [PubMed]
6. Ashrafi, O.; Yerushalmi, L.; Haghighat, F. Wastewater treatment in the pulp-and-paper industry: A review of treatment processes and the associated greenhouse gas emission. *J. Environ. Manag.* **2015**, *158*, 146–157. [CrossRef] [PubMed]
7. Hassaan, M.A.; El Nemr, A.; Hassaan, A. Health and environmental impacts of dyes: Mini review. *Am. J. Environ. Sci. Eng.* **2017**, *1*, 64–67.
8. Mashkoor, F.; Nasar, A. Polyaniline/Tectona grandis sawdust: A novel composite for efficient decontamination of synthetically polluted water containing crystal violet dye. *Groundw. Sustain. Dev.* **2019**, *8*, 390–401. [CrossRef]
9. Berradi, M.; Hsissou, R.; Khudhair, M.; Assouag, M.; Cherkaoui, O.; El Bachiri, A.; El Harfi, A. Textile finishing dyes and their impact on aquatic environs. *Heliyon* **2019**, *5*, e02711. [CrossRef] [PubMed]
10. Edokpayi, J.N.; Odiyo, J.O.; Durowoju, O.S. Impact of wastewater on surface water quality in developing countries: A case study of South Africa. *Water Qual.* **2017**, *10*, 66561. [CrossRef]
11. Collivignarelli, M.C.; Abbà, A.; Miino, M.C.; Damiani, S. Treatments for color removal from wastewater: State of the art. *J. Environ. Manag.* **2019**, *236*, 727–745. [CrossRef] [PubMed]

12. Bhatia, D.; Sharma, N.R.; Singh, J.; Kanwar, R.S. Biological methods for textile dye removal from wastewater: A review. *Crit. Rev. Environ. Sci. Technol.* **2017**, *47*, 1836–1876. [CrossRef]

13. Iwuozor, K.O. Prospects and challenges of using coagulation-flocculation method in the treatment of effluents. *Adv. J. Chem.-Sect. A* **2019**, *2*, 105–127. [CrossRef]

14. Särkkä, H.; Bhatnagar, A.; Sillanpää, M. Recent developments of electro-oxidation in water treatment—A review. *J. Electroanal. Chem.* **2015**, *754*, 46–56. [CrossRef]

15. Ma, W.; Zhang, M.; Liu, Z.; Kang, M.; Huang, C.; Fu, G. Fabrication of highly durable and robust superhydrophobic-superoleophilic nanofibrous membranes based on a fluorine-free system for efficient oil/water separation. *J. Membr. Sci.* **2019**, *570*, 303–313. [CrossRef]

16. Qing, W.; Shi, X.; Deng, Y.; Zhang, W.; Wang, J.; Tang, C.Y. Robust superhydrophobic-superoleophilic polytetrafluoroethylene nanofibrous membrane for oil/water separation. *J. Membr. Sci.* **2017**, *540*, 354–361. [CrossRef]

17. Zhu, Z.; Wu, P.; Liu, G.; He, X.; Qi, B.; Zeng, G.; Wang, W.; Sun, Y.; Cui, F. Ultrahigh adsorption capacity of anionic dyes with sharp selectivity through the cationic charged hybrid nanofibrous membranes. *Chem. Eng. J.* **2017**, *313*, 957–966. [CrossRef]

18. Mahmoud, M.E.; Nabil, G.M.; El-Mallah, N.M.; Bassiouny, H.I.; Kumar, S.; Abdel-Fattah, T.M. Kinetics, isotherm, and thermody-namic studies of the adsorption of reactive red 195 A dye from water by modified Switchgrass Biochar adsorbent. *J. Ind. Eng. Chem.* **2016**, *37*, 156–167. [CrossRef]

19. Wang, F.Y.; Wang, H.; Ma, J.W. Adsorption of cadmium (II) ions from aqueous solution by a new low-cost adsorbent—Bamboo charcoal. *J. Hazard. Mater.* **2010**, *177*, 300–306. [CrossRef]

20. Ho, Y.S.; McKay, G.A. comparison of chemisorption kinetic models applied to pollutant removal on various sorbents. *Process Saf. Environ. Prot.* **1998**, *76*, 332–340. [CrossRef]

21. Weber, W.J.; Morris, J.C. kinitics of adsorption on carbon from solution, J,of the sanitary Engineering division 1963, 89, 31–60.

22. Obradović, B. Guidelines for general adsorption kinetics modeling. *Hem. Ind.* **2020**, *74*, 65–70. [CrossRef]

23. Bouhamed, F.; Elouear, Z.; Bouzid, J. Adsorptive removal ofcopper(II) from aqueous solutions on activated carbon preparedfrom Tunisian date stones: Equilibrium, kinetics and thermody-namics. *J. Taiwan. Inst. Chem. Eng.* **2012**, *43*, 741–749. [CrossRef]

24. Wang, C.H.; Wen, W.C.; Hsu, H.C.; Yao, B.Y. High-capacitanceKOH-activated nitrogen-containing porous carbon material fromwaste coffee grounds in supercapacitor. *Adv. Powder Technol.* **2016**, *27*, 1387–1395. [CrossRef]

25. Dubinin, M.V.; Starinets, V.S.; Talanov, E.Y.; Mikheeva, I.B.; Belosludtseva, N.V.; Belosludtsev, K.N. Alisporivir improves mitochondrialfunction in skeletal muscle of mdx mice but suppresses mito-chondrial dynamics and biogenesis. *Int. J. Molec Sci.* **2021**, *22*, 9780. [CrossRef] [PubMed]

26. Torab-Mostaedi, M.; Ghaemi, A.; Ghassabzadeh, H.; Ghannadi-Maragheh, M. Removal of strontium and barium from aqueous solutions by adsorption onto expanded perlite. *Can. J. Chem. Eng.* **2011**, *89*, 1247–1254. [CrossRef]

27. Mohamad, A.D.M.; Abualreish, M.J.A.; Abu-Dief, A.M. Temperature and salt effects of the kinetic reactions of substituted 2-pyridylmethylene-8-quinolyl iron (II) complexes as antimicrobial, anti-cancer, and antioxidant agents with cyanide ions. *Can. J. Chem.* **2021**, *99*, 763–772. [CrossRef]

28. Owojori, O.J.; Reinecke, A.J.; Rozanov, A.B. Effects of salinity on partitioning, uptake and toxicity of zinc in the earthworm Eisenia fetida. *Soil. Biol. Biochem.* **2008**, *40*, 2385–2393. [CrossRef]

29. Seghier, A.; Habouchi, F.; Fortas, F.Z.; Cheklam, L.; Hadjel, M. Adsorption du bleu de sétapers issu de l'industrie de textile TAYAL de Relizane sur un biosorbant à faible coût préparé à base de feuilles d'artichaut. *Int. J. Nat. Resour. Environ.* **2021**, *3*, 61–72.

30. Kamran, U.; Bhatti, H.N.; Noreen, S.; Tahir, M.A.; Park, S.J. Chemically modified sugarcane bagasse-based biocomposites for efficient removal of acid red 1 dye: Kinetics, isotherms, thermodynamics, and desorption studies. *Chemosphere* **2022**, *291*, 132796. [CrossRef]

31. Makhlouf, M.; Hamacha, R.; Villiéras, F.; Bengueddach, A. Kinetics and thermodynamics adsorption of phenolic compounds on organic-inorganic hybrid mesoporous material. *Int. J. Innov. Appl. Stud.* **2013**, *3*, 1116–1124.

32. Bouberka, Z.; Kacha, S.; Kameche, M.; Elmaleh, S.; Derriche, Z. Sorption study of an acid dye from aqueous solutions using modified clays. *J. Hazard. Mater.* **2005**, *119*, 117–124. [CrossRef] [PubMed]

33. Abdellah, T. Etude de L'élimination du Chrome et de Bleu de Méthylène en Milieu Aqueux par Adsorption sur la Pyrophyllite Traitée et Non Traitée. Thèse Doctorale, Faculté des Sciences Rabat, Rabat, Morocco, 2006.

34. Temkin, M.J.; Pyzhev, V. Modifications récentes des isothermes de Langmuir. *Acta Phys. Chem.* **1940**, *12*, 217–222.

35. Freundlich, H. De l'adsorption des gaz. Section II. Cinétique et énergétique de l'adsorption des gaz. Article introductif à la section II. *Trans. Faraday Soc.* **1932**, *28*, 195–201. [CrossRef]

36. Chu, K.H. Revisiter l'isotherme de Temkin: Incohérence dimensionnelle et formes approximatives. *Rech. En. Chim. Ind. Et. Tech.* **2021**, *60*, 13140–13147.

37. Mahanty, B.; Behera, S.K.; Sahoo, N.K. Misinterpretation of Dubinin–Radushkevich isotherm and its implications on adsorption parameter estimates. *Sep. Sci. Technol.* **2023**, *58*, 1275–1282. [CrossRef]

38. Azzouni, D.; Baragh, F.; Mahmoud, A.M.; Alanazi, M.M.; Rais, Z.; Taleb, M. Optimization of methylene blue removal from aqueous solutions using activated carbon derived from coffee ground pyrolysis: A response surface methodology (RSM) approach for natural and cost-effective adsorption. *J. Saudi Chem. Soc.* **2023**, *27*, 101695. [CrossRef]
39. Azzouni, D.; Hassani, E.M.S.; Rais, Z.; Taleb, M. An Excellent Alternative to Industrial Activated Carbons for the Purification of Textile Water Elaborated from Waste Coffee Grounds. *Int. J. Environ. Res.* **2022**, *16*, 89. [CrossRef]